Accepted Manuscript

Effects of infiltration pressure on mechanical properties of Al-12Si/graphite composites for piston engines

J. Narciso, J.M. Molina, A. Rodríguez, F. Rodríguez-Reinoso, E. Louis

PII: S1359-8368(16)00055-X

DOI: 10.1016/j.compositesb.2016.01.022

Reference: JCOMB 3993

To appear in: *Composites Part B*

Received Date: 5 June 2015

Revised Date: 20 October 2015

Accepted Date: 6 January 2016

Please cite this article as: Narciso J, Molina JM, Rodríguez A, Rodríguez-Reinoso F, Louis E, Effects of infiltration pressure on mechanical properties of Al-12Si/graphite composites for piston engines, *Composites Part B* (2016), doi: 10.1016/j.compositesb.2016.01.022.

Effects of infiltration pressure on mechanical properties of Al-12Si/graphite composites for piston engines

J. Narciso[a,b], J. M. Molina[a,b], A. Rodríguez[a,b], F. Rodríguez-Reinoso[a,b], E. Louis[a,c,d],

[a]*Instituto Universitario de Materiales de Alicante, Universidad de Alicante, Apto 99, E-03080 Alicante, Spain.*
[b]*Departamento de Química Inorgánica de la Universidad de Alicante, Universidad de Alicante, Apto 99, E-03080 Alicante, Spain.*
[c]*Departamento de Física Aplicada, Universidad de Alicante, Apto 99, E-03080 Alicante, Spain.*
[d]*Unidad Asociada del Consejo Superior de Investigación Científicas, Universidad de Alicante, Apto 99, E-03080 Alicante, Spain*

ABSTRACT

In this work results for the flexural strength and the thermal properties of interpenetrated graphite preforms infiltrated with Al-12wt%Si are discussed and compared to those for packed graphite particles. To make this comparison relevant, graphite particles of four sizes in the range 15-124 μm, were obtained by grinding the graphite preform. Effects of the pressure applied to infiltrate the liquid alloy on composite properties were investigated. In spite of the largely different reinforcement volume fractions (90% in volume in the preform and around 50% in particle compacts) most properties are similar. Only the Coefficient of Thermal Expansion is 50% smaller in the preform composites. Thermal conductivity of the preform composites (slightly below 100 W/m.K), may be increased by reducing the graphite content, alloying, or increasing the infiltration pressure. The strength of particle composites follows Griffith criterion if the defect size is identified with the particle diameter. On the other hand, the composites strength remains increasing up to unusually high values of the infiltration pressure. This is consistent with the drainage curves measured in this work. Mg and Ti additions are those that produce the most significant improvements in performance. Although extensive development work remains to be done, it may be concluded that both mechanical and thermal properties make these materials suitable for the fabrication of piston engines.

Keywords: Metal Matrix composites (MMCs) A, Interphase B, Mechanical testing D, Liquid metal infiltration E.

1. INTRODUCTION

Among the materials families that are being developed for the fabrication of next generation piston engines, are the so-called interpenetrated composites IC [1-13]. Such a material is made up of two or more phases each one forming a three-dimensional (3D) connected network. It is pertinent noting here that it is not enough having as one of the phases a preform of high volume fraction of packed particles (PP) touching each other [14], but rather "physical" contact promoted for instance, by hot pressing [4,8], is required. Such important issue is discussed in detail in Ref. [4]. Although the number of phases in the IC is by no means limited, most developments have been focused on two phases IC. The number of material combinations and fabrication techniques of both the matrix preform and the composite is truly huge. Here we only comment a few that we have considered most pertinent to the present study [1-9]. As regards material combinations we here mention AlSiX/graphite [1-3], Al/SiC [4] and AlSiMg/SiC [5,6], TiC/Mg alloys [7], Alumina/Al [8], and Alumina/Ni [9]. Fabrication of the matrix has also deserved a lot of imagination: albeit hot pressing is the most popular, robotic deposition [8] or even wood precursors in the case of SiC [6] have been used. Composite fabrication in turn has been carried out by gas pressure infiltration [1,3,4,8], pressureless (or reactive) infiltration [5,7], squeeze casting [2], and hot pressing [9], among others.

In parallel to this wealth of experimental studies, a comparable theoretical activity is being developed [10-13]. In particular, a variety of bounds approaches [10,11] have been used, along with extensive micromechanical calculations [11,12]. Of special difficulty is the simulation of IC microstructure [11]. In this context it is worth mentioning the ever-increasing usefulness of three-dimensional X-ray micro-

tomography [13]. It is worth commenting the work on the "representative volume element size" reported in Ref. [13]. These authors concluded that present computational facilities does not allow to predict mechanical properties of IC from calculations based upon a single (large enough) region, but rather it is more practical and accurate, averaging over a large number of results derived from many calculations of small microstructures. Condensed matter scientists working on amorphous or disordered systems have followed this approach since many years by.

Let us comment in more detail those studies more related to the present work, namely, those on Al alloys/graphite [1-3] and that which compares performance of 3D and PP composites [4]. Graphite fully connected preforms have been gas pressure infiltrated with AlSiMg alloys concluding that preforms with lower porosity (10 vol%) led to composites showing a flexural strength 30% than that of IC based on preforms with a 13 vol% porosity. Etter et al [2] have carried out an in-depth investigation of the properties of graphite preforms/Al-Si using mechanically assisted high pressure infiltration showing that it was possible to meet the properties required to fabricate pistons for combustion engines (particularly of the Otto type). It has been also shown that infiltration of graphite preforms with Al-12Si eutectic alloy at 670ºC almost eliminate carbide formation [3]. Lin et al [4] have compared thermal properties of 3D and PP before and after being gas pressure infiltrated with liquid Al. They concluded that the 3D fully connected preforms had, before infiltration a Thermal Conductivity (TC) 10 times higher than PP preforms, while they had similar Coefficients of Thermal Expansion (CTE). Instead, after infiltration, IC had both TC and CTE higher than PP based composites (40% and 20% higher, respectively).

Actually, the properties that should show materials suitable for the just mentioned application are: 1) flexural strength higher than 150 MPa, 2) Coefficient of Thermal Expansion (CTE) below 12 ppm.K^{-1}, 3) Thermal Conductivity (TC) better than 100 W/m.K, and, 4) density below 2.5 g/cm^3. The material being used up to now is an Al-Si alloy with a high content of Si that typically shows the following properties: flexural strength 250 MPa, CTE 18-20 ppm.K^{-1}, density 2.8 g/cm^3 and TC 100 W/m.K.

Table 1. Average particle size D(4,3) in μm, and span [D(90)-D(10)]/D(50) of the particle size distribution, where D(x) is the diameter below which x percentage of particles is found. V_r is the reinforcement volume fraction, P_0 (kPa) is the minimum pressure to initiate infiltration (threshold pressure, taken from Ref. [14-16]) and P_b (bubbling pressure in kPa) and λ (exponent) are the two parameters that enter into Brooks and Corey equation (see Eq. (2)).

Reinforcement	D(4,3)	Span	V_r	P_0	P_b	λ
P1	15,1	1,39	0,51	1439	1526	5.92
P2	27,2	0,98	0,52	622	558	3.32
P3	64,0	0,95	0,52	283	130	0.95
P4	124,1	0,99	0,48	131	121	0.79
Preform	-	-	0,90	-	2177	2.88

In this work results for the mechanical and thermal properties of interpenetrated graphite preforms infiltrated with Al-12wt%Si, are presented and compared to those for packed graphite particles infiltrated with the same alloy. To make this comparison relevant, graphite particles of average diameters in the range 15-124 μm, were produced by grinding the graphite preform. Subsequent sieving was used to obtain the desired particle size. This procedure, although does not produce 3D preforms shows some of the topological features of the original 3D preform. Effects of the pressure applied to infiltrate the liquid alloy on composite properties, were also investigated. In spite of the largely different reinforcement volume fractions (90% in volume in the preform and around 50% in particle compacts) most properties are similar. The Coefficient of Thermal Expansion is 50% smaller in the IC. Thermal conductivity of the preform composites (slightly below 100 W/m.K), may be increased by reducing the graphite content, alloying, or increasing the infiltration pressure. The strength of particle composites follows Griffith criterion if the defect size is identified with the particle diameter. This is consistent with the brittle character of fracture that may nucleate at the particles/metal interface. In addition, the flexural strength remains increasing up to unusually high values of the infiltration pressure (between 3 and 30 times the threshold pressure, depending on particle size) probably due to the existence of porosity at many size scales. This is in line with the drainage curves measured in this work that show a slow increase of saturation with applied pressure. Note that in standard graphite or SiC particles saturation is reached for applied pressures lower than twice the threshold pressure [14-23]. The effects of a third alloying element was also investigated, concluding that Mg and Ti additions are those that produce the

most significant improvements in overall performance. These results allow concluding that both mechanical and thermal properties make these materials suitable for the fabrication of piston engines.

2. MATERIALS AND EXPERIMENTAL PROCEDURES

2.1 Materials

The porous interpenetrated graphite preforms (see Figure 1) used in this study were processed from needle coke as filler and coal-tar pitch as binder. Filler and binder were ground to the particle size required. This allows better control of the packing characteristics and optimizes the density and porosity of the final product. Filler and binder were blended in the proper proportion into a homogeneous mix where each filler particle was coated with the binder. This homogeneous mix was shaped or formed into preforms, green preforms, through isostatic molding, whereby external pressure was applied from all directions, resulting in a material with a great uniformity, isotropic properties and generally with few defects. The so obtained preforms were carbonized up to 1200 °C in inert atmosphere, where the volatile material was removed. Subsequently, the preforms were graphitized at 2500 °C in an inert atmosphere.

Graphite particles of four different sizes (15, 27, 64 and 124 μm, see Table 1) were used in this study. They were kindly supplied by Schunk Kohlenstofftechnik GmbH. In order to make comparison with composites based upon the preforms described above, particles were obtained by grinding those preforms and subsequently subjected to the sieving necessary to obtain the desired size. Particles, albeit highly irregular (see Figure 1), show a low overall aspect ratio (see Ref. [17]). The Al–12Si (hereafter Al–12Si) and Al-12Si-[4Mg, 1Ti, 1Cu, 4Sn and 2Pb] (hereafter Al-12Si-nX) alloys used to infiltrate the performs and the particle compacts were produced in our laboratories.

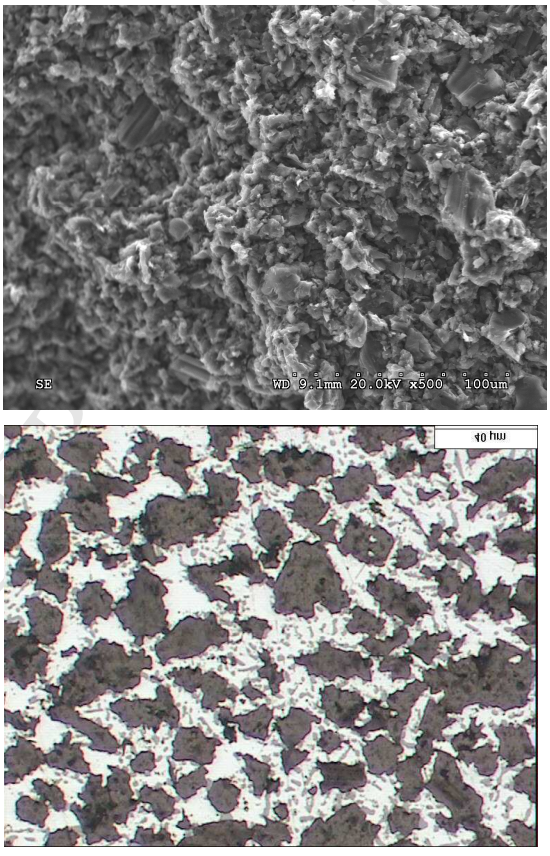

Figure 1. Optical micrographs of the as-received graphite preform (above) and of the particle P2 compact infiltrated (3 times the threshold pressure) with Al-12Si alloy.

2.2 Fabrication of composites.

Both, preforms and packed particles were gas pressure infiltrated with liquid Al-12Si alloys. Particles were packed within tubes of 16mm inner diameter having one of its ends closed. Preforms were also placed into those tubes. A piece of solid metal was placed inside the tube and on top of the graphite preform (or compact). Infiltration was carried out in a chamber described elsewhere [17,18]. Before heating, vacuum was applied until a pressure of 0.1 mbar was reached. Then the chamber was heated up to 640 ºC and pressurized at different pressures over threshold. The maximum pressure attained in this experiment was 4.2 MPa for particle composites, whereas the preform was infiltrated at 8 MPa. Pressure was maintained for 2 min and finally the system was cooled under pressure (see reference [17,18] for details). Pressures applied in this work are reported in Table 2. All are well above the respective threshold pressure (see Table 1).

The extent of metal filling was measured on each infiltrated sample by means of densitometry. Full drainage curves were also obtained in this work (see Ref. [15,16,24-26] for a detailed discussion of this issue).

2.3 Mechanical and thermal properties of the composites.

To measure the flexural strength, three-point bending tests were performed at room temperature on an Instron 4411 universal testing machine using a crosshead speed of 0.1 mm/min. All bending test samples were 4x8x32 mm in size, the distance between supports being 26 mm while the load was applied at the center of the specimen. Ten samples per composite were tested to verify the reliability of the material according to Weibull statistics (see Appendix). Hardness Rockwell C was carried out in a Zwick durometer, model ZHR4150AK.

Table 2. Physical properties of graphite/Al-12Si composite materials fabricated from both graphite particles compacts and graphite preforms (see also Table 1) at different infiltration pressures. TC and CTE stand for Thermal Conductivity and Coefficient of Thermal Expansion, whilst σ_f is the flexural strength.

Reinforcement	Pressure (kPa)	TC (W/m.K)	CTE ($x10^{-6}K^{-1}$)	σ_f (MPa)	Hardness (RC)	Density (g/cm^3)
P1	2360	89	14.7	115	67	2.27
	3130	90	14.9	112	72	2.32
	3700	92	15.1	150	80	2.33
	4200	104	15.6	178	92	2.36
P2	1070	97	13.8	111	55	2.19
	1390	99	14.3	130	63	2.26
	2100	105	14.3	128	64	2.29
	2650	107	14.4	138	62	2.30
	3320	111	14.4	141	67	2.31
	4200	112	14.5	150	71	2.33
P3	730	99	14.3	87	41	2.16
	980	101	14.4	91	45	2.17
	1580	106	14.4	112	53	2.21
	2190	108	14.7	113	59	2.26
	2800	107	14.8	146	67	2.26
	3300	109	14.7	157	71	2.27
	4200	120	15.4	160	73	2.32
P4	400	76	14.0	67	40	2.10
	1040	81	14.6	76	46	2.15
	1700	85	14.8	107	64	2.19
	2500	86	14.7	104	67	2.20
	3420	89	15.0	135	79	2.27
	4200	86	15.2	139	84	2.35
Preform	8000	97	8.0	121	66	2.17
	8000*	97	8.0	160	70	2.17

* Contact time graphite/liquid alloy: 1 s.

The thermal conductivity of the composites was measured by means of a relative steady-state (equal-flow) technique, in an experimental setup assembled at the laboratories of the Universidad de Alicante [21,23]. Sample and reference (preferentially cylindrical in shape) in contact across their (circular) cross sections, were clamped between a room temperature water-cooled block (reference end) and a block connected to a thermally stabilized hot water bath at 70 ºC (sample end). Losses through radiation and convection were neglected. The temperature gradient in the sample was measured, and compared to that in the reference, by means of two thermocouples in each of them. The linearity of the temperature gradient in the reference was measured, typically being within ±1%. We estimate the overall uncertainty of the measured thermal conductivities to be around ±5% (see Ref. [21,23]). Oxygen-free high purity copper (99.9998%), having a thermal conductivity at 40 ºC of 400 W/m.K, was used as reference. In the present case the reference was a cylinder of diameter of around 16 mm and length of 40 mm.

A thermo-mechanical analyzer (TMA 2940, TA Instruments) was used to obtain the thermal response curves from which the Coefficient of Thermal Expansion (CTE) was derived. Samples of 5 mm of length were cut from the infiltrated composites using a low speed saw, all of them being subsequently polished. Measurement were carried out applied force of 0.05 N, under nitrogen atmosphere, an in the temperature range 298-573 K (heating and cooling rates 3.0 $K.min^{-1}$). The samples were subjected to a least four heating and cooling cycles to remove large residual stress, if any, possibly developed during processing of the composite.

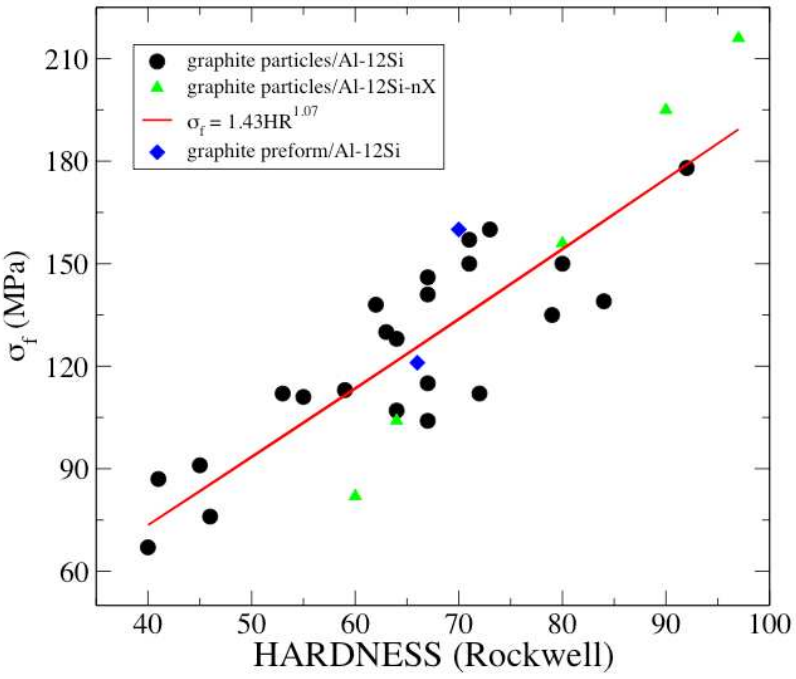

Figure 2. Flexural strength σ_f versus Rockwell hardness of graphite particles/Al-12Si-nX and graphite preform/Al-12Si composites fabricated by means of gas pressure infiltration at different applied pressures (see Tables 2 and 3). Although a rather large dispersion is observed, the experimental data reasonably admit a linear fit.

3. RESULTS AND DISCUSSION

3.1 Particle-based Composites

The main characteristics and properties (thermal and mechanical) of the particle-based composites fabricated and evaluated in this work are given in Tables 2 and 3. It is noted that both the CTE and the flexural strength improve as the applied pressure increases, i.e., the CTE decreases while the strength increases, albeit it is less noticeable in the former. Some conclusions relevant for the fabrication of the preform composites can be derived from the results of Tables 2 and 3. First it is noted that the CTE is never lower than 12 $ppm.K^{-1}$, which suggest that graphite content should be substantially increased. Best results are obtained at the highest applied pressures. Noting also that density is always below 2.5 g/cm^3, we may conclude that if there is any

possibility of reducing the CTE (for instance by increasing the particle content working with bimodal particle mixtures), these materials could be successfully used for the fabrication of piston engines.

Alloying with a third element does not improve significantly the overall performance of the composite (see Table 3). Mg and Ti are the additions that seem to be most promising. In the case of Ti, the thermal conductivity is lower than in the eutectic alloy (90 W/m.K compare to 105 W/m.K); however this could be easily improved by increasing the infiltration pressure. Varying the contact time (time in contact between graphite and the liquid alloy) may also improve the TC. Al-12Si-1Cu shows the highest mechanical properties, unfortunately both CTE and TC are rather poor.

3.1.1 Flexural strength versus hardness

It is interesting to check whether there is any relationship between the flexural strength and hardness. Fig. 2 shows a plot of the former against the latter for all materials fabricated in this work. Albeit there is a considerable dispersion, the overall aspect of the data and the fitting indicate that such a relationship does in fact exist. Actually, they are almost linearly related (note that the exponent of hardness is 1.07). This suggests, on the other hand, that the effect of residual porosity (which does also exist) is not significant. It should be here mentioned that a linear relationship between tensile strength and hardness was also reported in [27] for an Al alloy/SiC particles composites with particle contents higher than 10%.

Table 3. Physical properties of graphite/Al-12Si-nX composites. The composites have been manufactured at 3 times the threshold pressure. Graphite particle used to produce the compacts were 27 μm in average diameter (P2 of Table 1).

Alloys	Density (g/cm^3)	Hardness (RC)	σ_f (MPa)	CTE (10^{-6} K^{-1})	TC (W/m.K)
Al-12Si	2.31	64	128	14.4	105
Al-12Si-4Mg	2.31	80	156	14.0	104
Al-12Si-1Ti	2.35	90	195	12.8	90
Al-12Si-1Cu	2.37	97	216	14.4	78
Al-12Si-4Sn	2.36	60	82	15.9	106
Al-12Si-2Pb	2.35	64	104	15.5	108

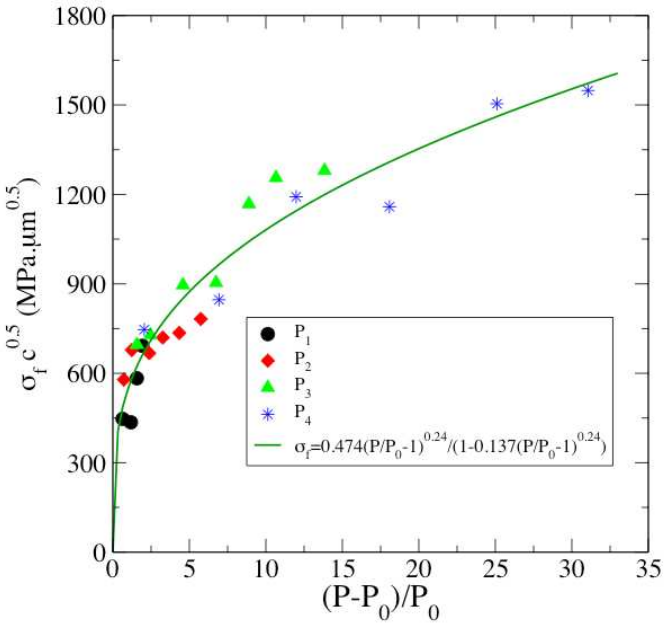

Figure 3. Flexural strength σ_f of compacts of graphite particles infiltrated with Al-12wt%Si alloy multiplied by $c^{0.5}$, c being the particle average diameter, versus the relative overpressure (P_0 being the threshold pressure) applied to infiltrate the liquid alloy.

3.1.2 Griffith's equation

All materials investigated here have low ductility, always lower than 2%. This, and fracture surfaces observed at the Scanning Electron microscope, indicate that fracture is always brittle. According to Griffith, when fracture is brittle, the material strength is determined by the size c of the defect or defects where fracture nucleates. In particular, Griffith derived the following expression [28],

$$\sigma_f = \frac{K_c}{c^{0,5}}\left(\frac{1}{Y}\right) \quad (1)$$

where σ_f is the fracture strength, K_c is the fracture toughness, and Y a geometric parameter related to the defect shape and the kind of fracture. Assuming that fracture is initiated at the particles/metal interface, we identify c with the average particle diameter. In order to check whether our results admit an interpretation in terms of Eq. (1) Fig 3 depicts $\sigma_f c^{1/2}$ versus the relative overpressure, i.e., $(P-P_0)/P_0$ for all particles and the eutectic alloy Al-12Si only. This is justified by the fact that changing the alloy significantly affects mechanical properties. It is interesting noting that the results for all four particles and different applied pressures coalesce reasonably over a single curve whose analytical form is given in the inset of Fig. 3. Had the factor $c^{1/2}$ not been included, curves for the four particles had been substantially different. This is so even though porosity differs appreciably among the composites based on the four particles of Table 1. The minimum porosity, which of course is attained at the maximum applied pressure, varies from 0.1 for particles P1 up to 2.6 for P4. This can be rationalized by noting that whenever there is relationship between the failure strength and mechanical properties (hardness in this case) one can safely assume that porosity plays a minor role.

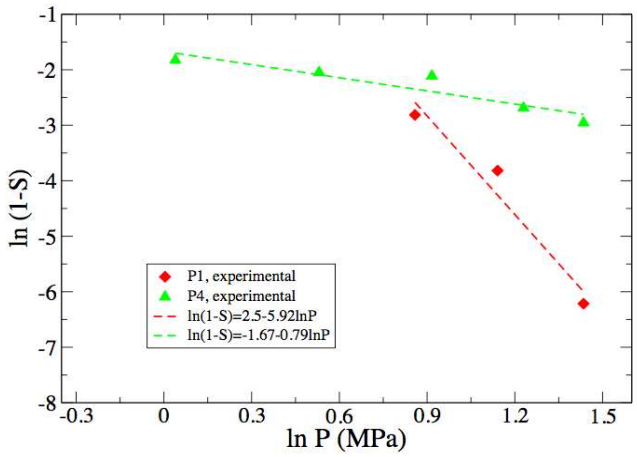

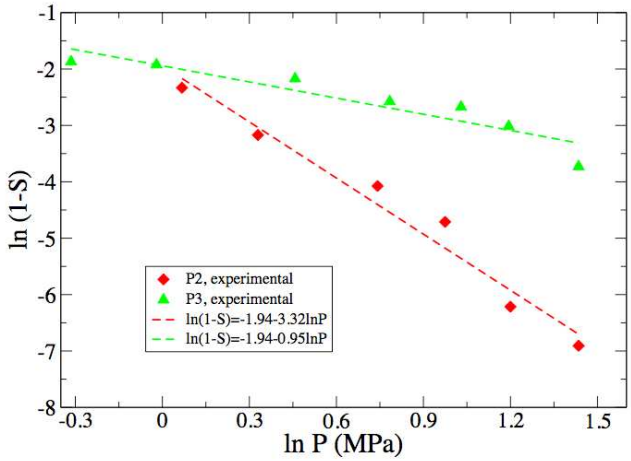

Figure 4. Representation of log(1−**S**) vs. log **P** for infiltration of Al–12Si into preforms made out of graphite particles

P1 and P4 (upper) and P2 and P3 (lower) of Table 1. The lines are least-square fittings of the experimental results with a linear regression coefficient better than 0.94. The derived Brooks and Corey parameters, see Eq. (2), are reported in Table 1.

The pressure dependence of the flexural strength up to very high values of the relative over-pressure, indicates that metal saturation in the present particle compacts is attained very slowly (note that in most systems full saturation is attained for relative overpressures less than 1). Thus, in order to support this hypothesis we measured the drainage curves for all particle compacts. According to Brooks and Corey [24-26], drainage curves can be described by means of the following semi-empirical law:

$$S = 1 - \left(\frac{P_b}{P} \right)^{\lambda} \qquad (2)$$

where P_b is a parameter, named bubbling pressure, defined as the minimum pressure necessary to create a continuous flow of metal in the perform, and the exponent λ is related to the pore size distribution and is typically given as an index of homogeneity in the pore structure of the preform. The information concerning the wetting properties of the system is contained in P_b. Results for compacts of all particles are shown in Figs. 3 and 4, while numerical values of λ and P_b are reported in Table 1. Saturation occurs far more slowly in particles P3 and P4 than in P1 and P2 (the exponent λ differs in a factor of three), in agreement with the results of Fig. 3. Such a low saturation kinetics is due to the highly irregular shape of graphite particles (Figure 1). It is interesting to note that the value of the exponent λ obtained in this works for P2 compacts is almost the same than that reported in Ref. [16] (3.4 to be compared to 3.32 in Fig. 3 of the present work). This is so despite of the fact that infiltrations in Ref. [15] were carried out at a maximum pressure of 1800 kPa, whereas in this work it was 4200 kPa (see Table 2). This supports the reliability of our experimental procedures.

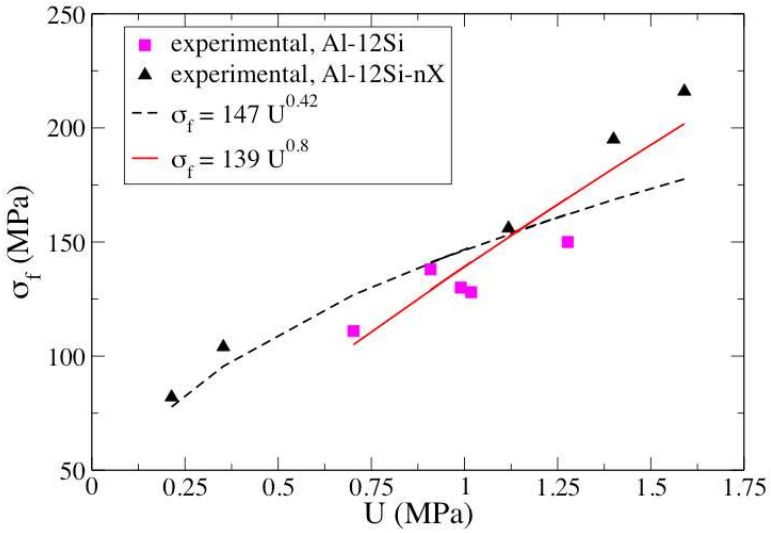

Figure 5. Flexural strength σ_f versus toughness modulus U (see Table 4) of composites fabricated by means of pressure infiltration of alloys Al-12Si-nX into compacts of graphite particles P2 of Table 1.

3.1.3 Flexural strength versus toughness modulus

A further checking of Griffith equation would be finding a relationship between the flexural strength and the stress intensity factor K. Unfortunately, the measurement of the latter is not feasible on the composite samples fabricated in this work. Thus, what we have done is to measure the modulus of toughness of

composites made out of particles P2, under the assumption that microstructure-related features would be similar. U was calculated by integration of the full flexural stress-strain curves. Experimental results are shown in Figure 5 and Table 4. Two power law fittings are explored, a fitting including all results (black broken line of Fig. 5) and a fitting excluding results for alloys Al-12Si-4Sn and Al-12Si-2Pb (red continuous line). The reason for excluding Sn and Pb alloys is that both elements when mixed with Al show a phase diagram with a miscibility gap and, as a consequence, they distribute through the aluminum matrix as minute balls of the pure element that may easily nucleate fracture. Excluding these elements, the fitting considerably improves approaching the linear relationship expected to hold for those two magnitudes. This is in our opinion a reasonable indication of the validity of Griffith equation in the present case.

3.2 Composites based on the interpenetrated graphite perform

The data obtained for the interpenetrated graphite preform/Al-12Si composite are also reported in Table 2. These composites fulfill the CTE requirement whereas their thermal conductivity is slightly below the required value (100 W/m.K). In addition, mechanical properties are good enough and the density is 5% lower than that of particle composites. These results suggest that a small decrease in the graphite content would likely be enough to produce a sufficient increase in the thermal conductivity. It is worth noting that decreasing the contact time (time of contact between graphite and the liquid alloy) from 2 min to 1 s, increases a 5% hardness and a 30% the flexural strength. This is an interface effect likely related to the irregular growth of the reaction products produced at long contact times. Finally note that the results for preform composites have also been included in Fig. 2. Clearly, the data lie within the range around the fitted straight line defined by the data for particle based composites.

Table 4. Toughness modulus U and infiltration pressure of composites made out of graphite particles P2 of Table 1 and the alloy indicated bellow.

Alloys	P (MPa)	U (MPa)
Al-12Si	1070	0.70
Al-12Si	1390	1.02
Al-12Si	2100	0.99
Al-12Si	2650	0.91
Al-12Si	4200	1.28
Al-12Si-4Mg	1800	1.12
Al-12Si-1Ti	2100	1.40
Al-12Si-1Cu	2100	1.59
Al-12Si-4Sn	1500	0.21
Al-12Si-2Pb	1500	0.35

4. CONCLUDING REMARKS

The results presented in this work allow concluding that graphite/Al-12Si-nX composites are good candidates for the fabrication of next generation pistons for combustion engines (particularly of the Otto type). Of course the present results can only be considered as preliminary and hard development work remains to be done. In particular, the effect of the contact time between graphite and the alloy in the liquid state has to be investigated in depth. In addition, the effects of a second alloying element deserve great attention. Although the results reported here suggest that Ti might be one of the most interesting additions to be considered, further investigations are required. Note that the addition of a second element not only affects the properties of the alloy but, what is likely more important, the characteristics of the graphite/metal interface.

Acknowledgements

The authors acknowledge financial support from the ‘‘Generalitat Valenciana’’ (PROMETEO II/2014/004- FEDER),

University of Alicante (Project GRE08-P13) and Spanish Ministry of Science and Innovation (MAT2011-25029). J.M. Molina also acknowledges the Spanish Ministry of Education and Culture for a ‘‘Ramón y Cajal’’ contract.

APPENDIX

Once checked that fracture is brittle, the reliability of the results has to be ensured. This requires a reasonably high number of tests to be done. In this work we carried out 9 additional tests for each particle compact all at an applied pressure three times the threshold pressure. In addition between 10 and 15 additional tests were carried out for the composites of graphite preforms at the conditions of Table 2. Data analysis is commonly done using Weibull distribution [29] that reads,

$$F(\sigma_c) = 1 - \exp\left(-\left(\frac{\sigma_c}{\sigma_0}\right)^m\right) \tag{3}$$

where $F(\sigma_c)$ is the probability that fracture occurs at a stress of σ_c. The exponent m is a parameter related to the dispersion of the experimental results, namely, the higher m, the smaller the data dispersion. Thus, this parameter characterizes the reliability of the data. Finally, σ_0 is the stress above which 63,2% of samples fail. Results for composites based upon particles P2 are shown in Fig.6. To facilitate the interpretation of the results and allow the calculation of the parameters in Eq. (3), a linear representation of Weibull distribution was used. The exponent m (see inset in Fig. 6) is high enough to guarantee the reliability of the testing and of the tested samples. Similar results were obtained for the rest of particle composites (based pon particles P1, P3 and P4) and in all cases the exponent m varied within the range 14-16.

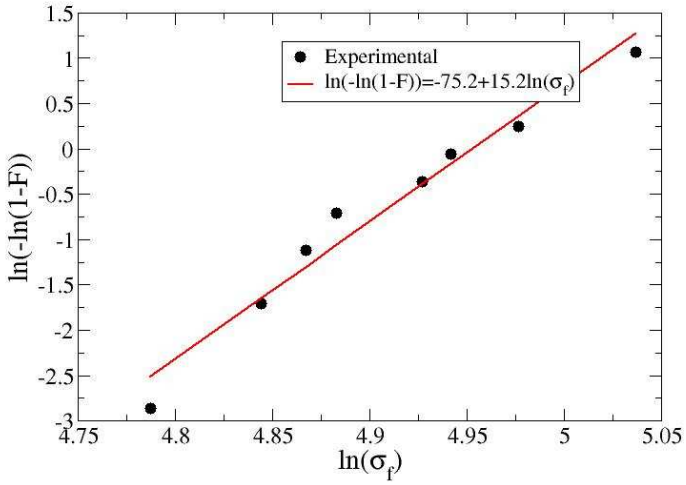

Figura 6. Weibull distribution (see Eq. (3)) for particle compacts P2 infiltrated with Al-12Si at three times the threshold pressure.

Results for the preform composites fabricated under the conditions of Table 2 are presented in Fig. 7. Similarly to what was done on particle composites, a statistical analysis of the experimental data was carried out. It is first noted that the exponent m of the preforms infiltrated with a contact time of 2 min almost is around 8. This value, albeit lower than that obtained for particle composites, is still rather high. However, when the contact time is reduced down to 1 s, m increases steeply up to 20, a value that is even higher than that obtained for particle composites. This result illustrates again the role of the interface, as during a long contact time reaction at the metal/graphite interface may modify its properties in an irregular manner.

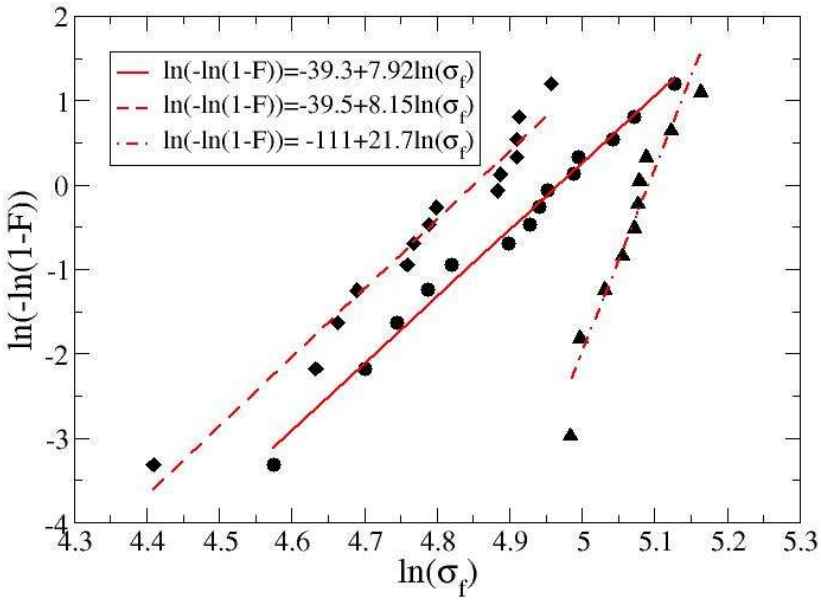

Figure 7. Weibull distribution (see Eq. (3)) for graphite preforms infiltrated with Al-12Si at 4500 MPa (circles), 8000 MPa (diamonds) with a contact time (see text) of 2 min, and 8000 MPa but with a contact time of 1s (triangles).

REFERENCES

[1] Etter T., Papakyriacou M., Schulz P., Uggowitzer P.J., Mechanical and Thermophysical Properties of Graphite/Al Composites produced by Casting Infiltration Methods. Carbon 2003;41:1017-1024.

[2] Etter T., Kuebler J., Frey T., Schulz P., Löfler JF., Uggowitzer PJ. Strength and Fracture Toughness of Interpenetrating graphite/aluminium Composites Produced by Indirect Squeeze Casting Process. Materials Science & Engineering 2004;A386:61-67.

[3] Etter T., Schulz P., Weber M., J. Metz J., Wimmler M., L¨offler J.F., Uggowitzer P.J. Aluminium carbide formation in interpenetrating graphite/aluminium composites. Materials Science and Engineering A 2007; 448: 1–6.

[4] Lin S, Xiong D, Liu M., Bai S., Zhao X. Thermophysical properties of SiC/Al composites with three dimensional interpenetrating network structure. Ceramics International 2014; 40: 7539–7544.

[5] Shaga A., Shen P., Sun C., Jiang Q. Lamellar-interpenetrated Al–Si–Mg/SiC composites fabricated by freeze casting and pressureless infiltration. Materials Science & Engineering A 2015; 630: 78–84.

[6] Wilkes T.E., Young M.L., Sepulveda R.E., Dunand D.C., Faber K.T. Composites by aluminum infiltration of porous silicon carbide derived from wood precursors. Scripta Materialia 2006; 55: 1083–1086.

[7] Chen L., Guo J., Yu B., Ma Z. Compressive Creep Behavior of TiC/AZ91D Magnesium-matrix composites with Interpenetrating Networks. J. Mater. Sci. Technol. 2007; 23:207-212.

[8] San Marchi C., Kouzeli M., Rao R., Lewis J.A., Dunand D.C. Alumina–aluminum interpenetrating-phase composites with three-dimensional periodic architecture. Scripta Materialia 2003; 49: 861–866.

[9] Aldrich D.E., Fan Z. Microstructural characterisation of interpenetrating nickel/alumina composites. Materials Characterization 2001; 47: 167– 173.

[10] Torquato S., Yeong C.L.Y., Rintoul M.D., Milius D.L., Aksay I.A. Elastic Properties and Structure of Interpenetrating Boron Carbide/Aluminum Multiphase Composites. J. Am. Ceram. Soc. 1999; 82: 1263–1268.

[11] Wegner L.D., Gibson L.J. The mechanical behaviour of interpenetrating phase composites-I: modelling. International Journal of Mechanical Sciences 2000; 42: 925-942.

[12] Feng X-Q, Mai Y.W., Qin Q-H. A micromechanical model for interpenetrating multiphase composites. Comp. Mater. Sci. 2003; 28: 486–493.

[13] Heggli M., Etter T., Wyss P., Uggowitzer P.J., Gusev A.A. Approaching representative volume size in interpenetrating phase composites. Advanced Eng. Mater. 2005; 7: 225-229.

[14] Rodríguez-Guerrero A., Sánchez S.A., Narciso J., Louis, E., Rodríguez-Reinoso F., Pressure Infiltration of Al-12 wt% Si-X (X=Cu, Ti, Mg) alloys into graphite particle performs. Acta Materialia 2006;54:1821-1831.

[15] Molina JM., Rodríguez-Guerrero A., Bahraini M., Weber L., Narciso J., Rodríguez –Reinoso F., Louis E., Mortensen A., Infiltration of graphite preforms with Al-Si eutectic alloy and mercury. Scripta Materialia 2007;56:991-994.

[16] Rodríguez-Guerrero A., Molina JM., Rodríguez-Reinoso F., Narciso J., Louis E. Pore filling in graphite particle compacts infiltrated with Al–12 wt.%Si and Al–12 wt.%Si–1 wt.%Cu alloys. Materials Science and Engineering 2008;A495**:**276-280.

[17] García-Cordovilla C., Louis E., Narciso J., Pressure infiltration of packed ceramic particulates by liquid metals. Acta Materialia 1999;47:4461-4479.

[18] Molina J.M., Saravanan R.A., Arpón R., García-Cordovilla C., Louis E., Narciso J. Pressure infiltration of liquid aluminium into packed SiC particulate with a bimodal size distribution. Acta Materialia 2002; 50: 247–257.

[19] Sánchez S.A., Rodríguez-Guerrero A., Narciso J., Louis, E., Rodríguez-Reinoso F., Pressure Infiltration of Al an Al-Si alloys into carbon particulate compacts. Journal of Materials Science 2005;40(9-10):2519-2522.

[20] Molina JM., Arpón R., Saravanan RA., García-Cordovilla C., Louis E., Narciso J. Threshold pressure for infiltration and particle specific surface area of particle compacts with bimodal size distributions. Scripta Materialia 2004;5:623-626.

[21] Prieto R., Molina JM., Narciso J., Louis E. Thermal Conductivity of graphite flakes-SiC particles/metal composites. Composites Part A 2011;42:1970-1977.

[22] Prieto R., Molina JM., Narciso J, Louis E. Fabrication and properties of graphite flakes/metal composites for thermal management applications. Scripta Materialia 2008;59:11-14.

[23] Molina J.M., Prieto R., Narciso J., Louis E. The effect of porosity on the thermal conductivity of Al–12 wt.% Si/SiC composites. Scripta Materialia 2009;60:582-585.

[24] Molina J.M., Narciso J., E. Louis E. On the triple line in infiltration of liquid metals into porous preform. Scripta Materialia 2010;62;961-965.

[25] Bahraini M, Molina JM., Kida M., Weber L., Narciso J., Mortensen A. Measuring and tailoring capillary forces during liquid metal infiltration. Current Opinión in Solid State & Materials Science 2005;9:196-201.

[26] Michaud V., Mortensen A. Infiltration processing of fibre reinforced composites: governing phenomena. Composites Part A 2001;32:981-996.

[27] Shen Y.-L., Williams J.J., Piotrowski G., Chawla N., Guo Y.L. Correlation between tensile and indentation behavior of particle-reinforced metal matrix composites: an experimental and numerical study. Acta Materialia 2001;49:3219-3229.

[28] Callister W.D. Jr, Materials Science and Engineering, An Introduction 7th ed, John Wiley & Sons, New York , USA, 2007.

[29] Weibull W. A Statiscal distribution function of wide applicability. ASME Journal of Applied Mechanics 1951; 18:293-297.